

REPORT DOCUMENTATION PAGE

Form Approved
OMB NO. 0704-0188

Public Reporting burden for this collection of information is estimated to average 1 hour per response, including the time for reviewing instructions, searching existing data sources, gathering and maintaining the data needed, and completing and reviewing the collection of information. Send comment regarding this burden estimates or any other aspect of this collection of information, including suggestions for reducing this burden, to Washington Headquarters Services, Directorate for information Operations and Reports, 1215 Jefferson Davis Highway, Suite 1204, Arlington, VA 22202-4302, and to the Office of Management and Budget, Paperwork Reduction Project (0704-0188,) Washington, DC 20503.

1. AGENCY USE ONLY (Leave Blank)		2. REPORT DATE 5/30/2008	3. REPORT TYPE AND DATES COVERED Final Report August 1 2007 to April 30, 2008	
4. TITLE AND SUBTITLE High Current Density Cathodes for Future Vacuum Electronics Applications			5. FUNDING NUMBERS FA9550-07-C-0063	
7. PERFORMING ORGANIZATION NAME(S) AND ADDRESS(ES) Calabazas Creek Research, Inc. 690 Port Drive, San Mateo, CA 94404 Massachusetts Institute of Technology 77 Massachusetts Ave. E-19-750 Cambridge, MA 02139			8. PERFORMING ORGANIZATION REPORT NUMBER	
9. SPONSORING / MONITORING AGENCY NAME(S) AND ADDRESS(ES) USAF, AFRL AF Office of Scientific Research 875 North Randolph Street, RM 312 Arlington, VA 2220			10. SPONSORING / MONITORING AGENCY REPORT NUMBER	
11. SUPPLEMENTARY NOTES The views, opinions and/or findings contained in this report are those of the author(s) and should not be construed as an official Department of the Air Force position, policy or decision, unless so designated by other documentation.				
12 a. DISTRIBUTION / AVAILABILITY STATEMENT Approved for public release; distribution unlimited.			12 b. DISTRIBUTION CODE	
13. ABSTRACT (Maximum 200 words) This final report summarizes the achievements at Calabazas Creek Research, Inc. and Massachusetts Institute of Technology to develop and demonstrate techniques for fabricating high current density cathodes using scandium to lower the emission work function. Several techniques were investigated for depositing scandium on and beneath the surface of cathode emitters with techniques for replenishing that removed by normal surface erosion processes. Results indicate that several techniques can successfully provide the initial deposition and subsequent replenishment for long lifetime operation. The techniques use readily available fabrication capabilities. A photonic band gap traveling wave circuit was designed compatible with an electron gun incorporating the high current density capability. Such a device would demonstrate the effectiveness of scandate cathodes in typical RF sources.				
14. SUBJECT TERMS Cathodes, electron emitter, scandate, scandium, electron gun, CVD, CVI, TWT			15. NUMBER OF PAGES 24	
			16. PRICE CODE	
17. SECURITY CLASSIFICATION OR REPORT UNCLASSIFIED	18. SECURITY CLASSIFICATION ON THIS PAGE UNCLASSIFIED	19. SECURITY CLASSIFICATION OF ABSTRACT UNCLASSIFIED	20. LIMITATION OF ABSTRACT UL	

NSN 7540-01-280-5500

Standard Form 298 (Rev.2-89)
Prescribed by ANSI Std. Z39-18
298-102

**High Current Density Scandate Cathodes
for Future Vacuum Electronics Applications**

USAF/AFRL Contract Number FA9550-07-C-0063

Final Report

Calabazas Creek Research, Inc.
690 Port Drive, San Mateo, CA 94404
(650) 312-9575
RLI@CalCreek.com
www.CalCreek.com

May 30, 2008

Glossary

RF	Radio Frequency
CCR	Calabazas Creek Research, Inc. - small business proposer
CPI	Communications & Power Industries, Inc. - subcontractor
MIT	Massachusetts Institute of Technology
HFSS	Ansoft Corporation's High Frequency Structure Simulator
TWT	Traveling Wave Tube - device for generating high levels of RF power
DARPA	Defense Advanced Research Agency
PBG	Photonic band gap
W-Band	75-111 GHz
dB	Decibels
GHz	10^6 Hz
SEM	Scanning electron microscope
EDAX	Energy Dispersive X-ray Analysis
TWT	Traveling Wave Tube
MEMS	micro-electro-mechanical systems
EIK	Extended interaction klystron

1. Introduction

All RF vacuum electron sources require a high quality electron beam for efficient operation. Research on improved cathodes is constantly exploring new alternatives for producing these beams. The goal is to produce high current density, uniform electron beams with long life. Presently, only thermionic dispenser cathodes are practical for high power RF sources. Typical thermionic cathodes consists of a tungsten matrix impregnated with a mixture of barium oxide, calcium oxide and aluminum oxide that reduces the work function of the tungsten surface. These cathodes typically operate around 1000° C.

In the late 1980s, researchers reported cathode work function reduction using scandium. Two groups presented improved performance, including one led by J. Hasker at Phillips Research Laboratories in the Netherlands [1] and S. Yamamoto in Japan [2]. Hasker et al. started with a typical tungsten matrix that was lightly pre-pressed. On top of this, they placed an additional layer consisting of tungsten and 5% wt. Sc_2O_3 . The configuration was then pressed and sintered between 1500-2000° C. This was called a 'Top-Layer Scandate Cathode.' The top layer was approximately 0.4 mm thick and was impregnated with barium aluminate in a 4:1:1 molar ratio of $\text{BaO}:\text{CaO}:\text{Al}_2\text{O}_3$. In practice, the barium and barium oxide activate the scandium oxide/tungsten surface.

Yamamoto et al used a standard tungsten matrix cathode with a sputter coated layer of tungsten containing varying amounts of Sc_2O_3 . Activation resulted in a thin film of monatomic order consisting of Ba, Sc, and O. The thin film contained about 5% Sc_2O_3 .

Each group reported significantly improved performance over standard impregnated cathodes. Hasker et al reported improved performance over the Yamamoto-type cathode following ion bombardment, which is a routine occurrence in video applications for which the cathodes were intended. It appears that scandium becomes relatively immobile following initial activation and is not easily replaced following removal from whatever mechanism. Once the film containing the scandium was removed from the Yamamoto-type cathode, it could not be easily replaced by additional scandium below the surface. Since the scandium was constituent in the top layer cathode, the reduced mobility was not as much of an issue, though some degradation was observed.

While the top-layer approach appeared more beneficial in resisting degradation from ion bombardment, it could present problems for cathodes in RF sources where spherical shaped cathodes are used to achieve beam compression. It could be difficult to maintain the thin layer of tungsten and Sc_2O_3 matrix when machining of the surface as required to achieve the proper curvature. This would not be as serious a problem for the Yamamoto-type cathode, since the thin layer could be sputtered on following machining.

The Phase I program explored techniques for depositing much thicker layers of scandium than achieved by Yamamoto. (*Note, in this report, scandium and scandium oxide will be used interchangeably. It should be noted that scandium will convert to scandium oxide in the presence of air, to which all cathodes will be exposed.*) The techniques would not only deposit material on the surface, but allow deposition into the pores of the cathode, providing substantial subsurface scandium available for replenishing that lost from the surface. This represents a combination of the Hasker and Yamamoto approaches, though with all the scandium deposited on and just below the surface. This would provide sufficient scandium at the emission surface to survive removal processes for the anticipated life of the cathode. The processes developed in Phase I would be applied to cathode surfaces following machining operations to shape the emission surface. This will be described in more detail in Section 2.

In 1990, Lesny and Forman reported on studies of the surface chemistry of scandate cathodes [3]. This research was instrumental in identifying the importance of barium oxide in providing oxygen for the scandium on the surface. They definitively showed that barium alone did not result in improved cathode performance while improvements were observed with barium oxide absorbate on a scandium substrate. Even at elevated temperatures, they could not get barium to react with or absorb on a scandium surface. These results appear to indicate that it was barium oxide on scandia that was responsible for the improved performance.

They suggested a model for explaining the operation of the top-layer scandate cathode, illustrated in Figure 1. During operation, barium loss is replenished by reaction of the impregnate with the tungsten. This is similar to conventional impregnated cathodes. Scandia is a high electrical resistivity material, and the surrounding tungsten acts as a current path around the scandia crystal and permits high electron current emission from the barium oxide on the scandia surface.

Crombeen and Hasker reported on similar studies at the same time [4]. They indicated that a Ba/Sc/O surface monolayer complex on the tungsten is essential for copious emission. They also indicated that the oxygen content of the coverage must remain below certain limits, since the electro-negativity of excess oxygen could lead to an increase in the work function. An issue continued to be replenishment of the scandium on the surface following ion bombardment. Hasker et al concluded that it is unlikely that the scandium can be transported to the cathode surface as a scandium and tungsten containing compound [5].

Raju and Maloney applied a semiconductor model to impregnated scandate cathodes to explain the improved performance [6]. Application of a patch field treatment showed that the nonsaturation of current-voltage characteristics was not primarily due to an inherent patchy behavior. The semiconductor model required the active material to have a depth substantially greater than that of a mature B-type cathode. Their analysis showed how the depth and doping density affect the calculated field enhancement. Theoretical and experimental studies indicated that the scandate cathode surface is composed substantially of thick patches that play a dominant role in emission. The high emission from these patches is due to formation of a layer rather than a particular structure. This might explain why possible removal of these layers by ion bombardment leads to permanent degradation of the emission.

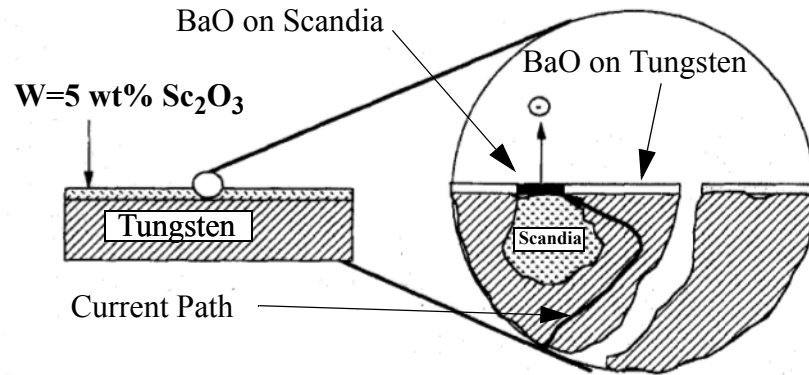


Figure 1. Surface model for top-layer scandate cathode proposed by Lesny and Forman

More recently, Gaertner and Baratt at Phillips Research Laboratories reported on life-limiting mechanisms in scandate cathodes [7]. It appears their studies were confined to the top-layer cathodes promoted by Phillips. Assuming no loss of scandium from the surface, end of life occurs when Ba diffusion through the porous matrix falls below BaO evaporation from the surface, as with conventional thermionic cathodes.

Issues with replenishment of scandium on the surface following removal by ion bombardment was confirmed by Shih et al at the Naval Research Laboratory [8]. They noted that replenishment mechanisms of scandium in the chemical environment of the present scandate cathodes is unlikely to be efficient and may require additives to lower the decomposition temperature of Sc_2O_3 , which is higher than practical cathode temperatures.

In the Phase I program, Calabazas Creek Research (CCR) explored an alternative technique. The Phase I approach investigated incorporation of scandium into tungsten wire cathodes developed by CCR during a previous research program [9]. Tungsten wire cathodes incorporate the barium calcium aluminate compound in a reservoir between the emission surface and the cathode heater. Consequently, the reservoir temperature is considerably higher than the emission surface. The Phase I approach explored inclusion of scandium in the reservoir. The expectation is that the higher temperature will decompose Sc_2O_3 and allow scandium transport to the surface with the barium compound. If the temperature is sufficiently high and the scandium propagates through the pores to the emission surface, this technique could be quite efficient.

More recently, the center for scandate cathode research has shifted to the Peoples Republic of China. At the 5th International Vacuum Electron Sources Conference in 2004, scandate papers were presented from four different research centers. Zhang et al from the Institute of Electronics in Beijing reported on recovery characteristics following ion bombardment [10]. Liu et al from the Key laboratory of Advanced Function Materials Ministry of Education, School of Materials

Science and Engineering in Beijing presented an operating model for scandate cathodes with scandia doped tungsten particles [11]. Jiang et al at Beijing Kedian Microwave Electronic Co. Ltd. discussed the preparation of scandate cathodes and their application [12]. Wang Shuguang at Chengdu Guoguang Electric Co. Ltd. discussed potential improvements in the uniformity of emission and the emission current density [13].

A major advanced may have been accomplished in China by developing a technique for creating and sintering sub-micron particles of tungsten and scandium [14]. Yuan reported on two methods called liquid-solid doping and liquid-liquid doping to create nanometer scale particles. Rhenium was added to further reduce the size of the tungsten grains. The doped tungsten powder was pressed and sintered into porous matrices approximately 3 mm in diameter and 1 mm thick and impregnated with a molar ratio of 4:1:1 of barium calcium aluminates. Emission properties were tested using a close-spaced diode configuration. Because of the small size of the tungsten grains, conventional fabrication processes for pressing and sintering were not applicable. The paper does not describe the required process, but reported it was developed experimentally. Typically, the smaller the grain size, the greater the force required for pressing. Previous experiments with micron size tungsten grains in the U.S. was limited by the capability of pressing equipment available to cathode manufacturers.

Several of the Chinese cathodes were provided to the Stanford Linear Accelerator Center (SLAC) for testing. Glenn Schietrum confirmed that emission densities approaching 100 A/cm^2 could be achieved [15], and the lifetime of these cathodes is still being investigated. SLAC uses scandate cathodes in klystrons for their linear accelerator with excellent results. Current densities are less than 10 A/cm^2 , however, so these results may not be applicable for higher current density operation [19].

Researchers at the Microwave Tube Research & Development Center in India are working with mixed metal matrix cathodes where 3% scandium oxide is added to a 5:3:2 molar ratio of the barium calcium aluminates impregnant [16]. The porous metal cathode consists of a mixture of tungsten and iridium. They achieved work function values ranging from 1.7 to 1.93 with emission densities up to 54 A/cm^2 . They reported that the surface coverage of scandium was typical of other scandate cathodes.

It seems clear that duplicating the nano-particle fabrication process and the advanced pressing and sintering capability achieved in China is far beyond the resources of an STTR program. Therefore, CCR and MIT explored different approaches that build on existing research in controlled porosity cathodes. CCR was funded by the U.S. Department of Energy to develop reservoir cathodes by sintering tungsten wires to form a uniform matrix of pores through the material [9, 17]. Figure 2 shows a cross section of the material with a uniform distribution of pores through the tungsten. Additional information on this program is provided in reference 9.

As previous research demonstrated, high current density emission requires Sc_2O_3 on the cathode surface. While this is relatively simple to achieve for new cathodes, the material is not easily replaced following

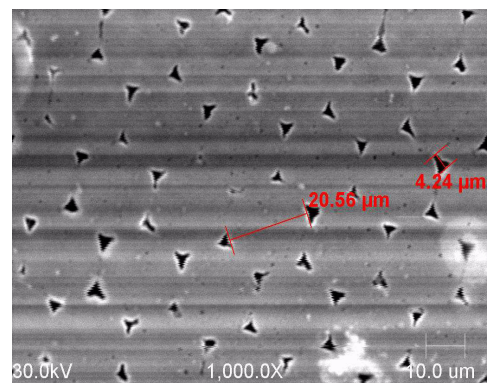


Figure 2. Cross section of sintered tungsten formed by 20 micron diameter wires

removal by various processes, such as ion bombardment. Previous cathodes exhibited an unrecoverable degradation in performance. The fundamental cause is the lack of mobility of scandium in porous tungsten cathodes. The Phase I program investigate three techniques to provide scandium on the cathode surface, even when subjected to removal processes.

M. Feinlab at Varian Associates investigated incorporating scandium into the impregnate in 1985 [21]. Feinlab obtain substantial improvement in cathode performance using a 3:1:1 impregnant with scandium. Note that researchers in India are using a 5:3:2 impregnant with scandium [16]. The expectation is that barium diffusion through the pores to the surface will bring scandium particles to the surface also. During initial operation, this appeared to operate as expected, but as the surface scandium is depleted or removed, the material must diffuse from deeper in the matrix. It is conceivable that as this transport distance become longer, there is greater opportunity for the scandium to be deposited on tungsten below the surface where it becomes bound and can not contribute to cathode emission. An advantage with reservoir cathodes is that the porous material only forms a thin cap over a large reservoir of the barium calcium aluminates mixture. Therefore, there is always a relatively short transport distance to the cathode surface. Even if scandium particles attach to tungsten particles within the cap, there is the possibility that the tungsten may become saturated so that no further binding occurs, allowing the following material to reach the surface. The Phase I program explored this approach.

A second technique uses scandium as a braze material to bind the tungsten wire structure. Initially it was proposed to sinter alternating scandium and tungsten wires; however, scandium melts at approximately 1630° C, while temperatures over 2000° C are required to sinter tungsten. The brazing approach appears to work well, however, and some scanning electron microscope photographs of a brazed structure are presented in Section 2.

Recall the model proposed by Lesny and Forman and illustrated in Figure 1. If this is, indeed, the true model, then the brazing configuration would be close to ideal, since scandium would be a fundamental constituent of the emission surface coating the interior of the pores and the interface between the tungsten wires. BaO diffusing through the pores would react at the tungsten-scandium interface to release oxygen to form Sc_2O_3 . Such a structure could provide extremely uniform emission with a high current density. The reservoir supply of barium/scandium would insure very long life.

Discussions with one of our industrial partners resulted in an additional approach, alluded to earlier. This involves deposition of scandium onto the cathode structure such that substantial penetration occurs into the pores. A final machining of the surface would remove the surface scandium and re-expose the tungsten structure. The resulting surface would then be tungsten with a layer of scandium between the pores and the tungsten. This would again provide the required configuration described by Lesny and Forman.

The results from the Phase I program indicate that each proposed approach is feasible. These results will be described in detail in Section 2.

2. Phase I Technical Results

The Phase I objective was to demonstrate feasible, practical, cost-effective techniques for producing long life, high current density, scandate cathodes. The results indicated that three techniques are feasible and are provided below.

Task 1. Investigate diffusion of scandium doped impregnant from the reservoir to the emission surface of a sintered tungsten wire cathode.

CCR's sintered tungsten wire cathodes contain a thin cap of sintered tungsten with a regular array of pores of uniform size and length. This allows precise control of the barium diffusion rate. Details of the construction were presented in the Phase I proposal, as well as a photograph of the prototype cathode, shown here in Figure 3. To verify adequate diffusion of barium through the cap, the cathode was installed in a test device at Communications & Power Industries, Inc. This device consists of a support structure inside a vacuum chamber with a quartz crystal located a short distance from the emitter. As the cathode is heated and barium evaporates from the surface, the deposition on the quartz crystal changes the frequency of a precision oscillator. The change in frequency can then be correlated with the diffusion rate of barium to the surface. The results are shown in Figure 4. These measurements were taken at the nominal operating temperature for the cathode and indicate that barium diffusion is consistent with cathode operation exceeding 20 A/cm^2 . The cathode is now being installed in a gun stem for high voltage testing.

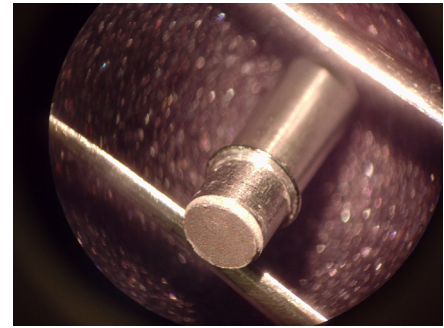


Figure 3. Reservoir cathode with sintered tungsten wire cap. Diameter of the emitter is 0.150 inches.

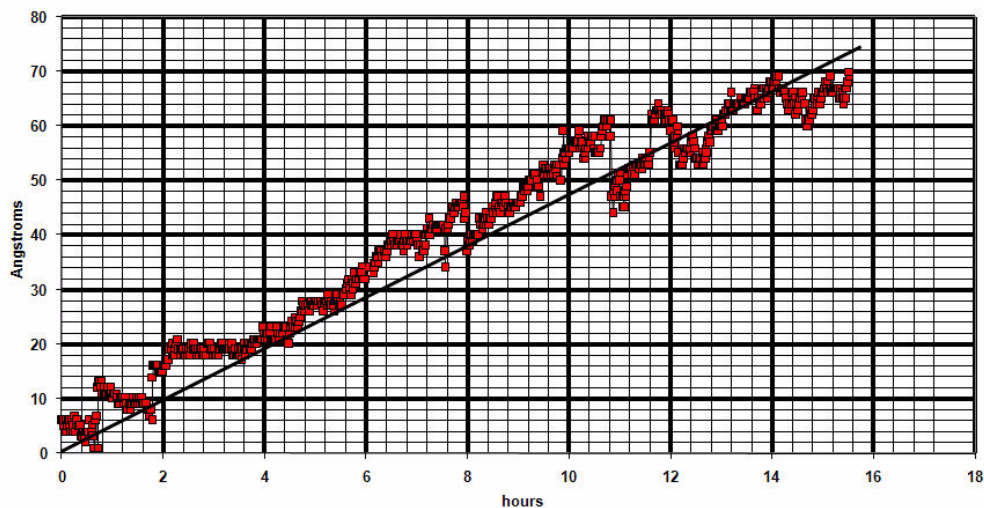


Figure 4. Measured barium diffusion from tungsten wire cathode

As mentioned above, a fundamental problem with scandate cathodes is replenishment of scandium particles on the emitter surface. These particles are routinely removed by back ion bombardment and other processes during normal cathode operation. Consequently, previous scandate cathodes exhibited decreased performance with time.

The goal of this task was to determine if scandate replenishment could be achieved by including scandium in the reservoir material and transporting it to the surface with the barium compound. Previous attempts to use this process in non-reservoir, porous tungsten cathodes failed due to the lack of mobility of the scandium. It appears that scandium adheres to tungsten within the porous structure and cannot then be moved to the emitter surface. Since scandium will be stored within the reservoir, rather than in porous tungsten, it is anticipated that it will transport through the thin cap along with the barium without contact with the tungsten until it reaches the emitter surface. The cap on the prototype emitter is approximately 0.025 in thick.

CCR located a distributor for scandium powder and procured 100 grams. The powder was received near the beginning of October and metallurgically analyzed. The material is 99% scandium and consists of particles approximately 50 microns in diameter. The pore size in CCR's prototype cathode is approximately 4 microns in cross section; consequently, the particles would be too large for this cathode. That cathode was constructed using 20 micron diameter tungsten wire. Larger pore size can be achieved by using larger diameter tungsten wire, which will also facilitate the fabrication. The advantage of the tungsten wire approach is that the pore size can be easily controlled, unlike in powdered tungsten cathodes.

Figure 5 shows the relationship between the wire size and the pore size. The larger circles represent a cross section of the wire, and the smaller circle represents the clear diameter of the pores. Figure 5 indicates that 400 micron diameter wire will allow passage of 50 micron diameter particles.

Ultimately, it would be necessary to obtain smaller size scandium powder to allow the smaller pore size. This would allow more uniform deposition of the scandium and barium over the emission surface. The large pore size would also result in excessive barium transport to the surface. This would result in reduced lifetime and possible deposition of barium on electrode surfaces.

In the Phase I program, an attempt was made to fabricate a tungsten wire cathode with these characteristics. Figure 6 shows a photograph of a section of sintered tungsten wires for the test device. This structure uses tungsten wire approximately 0.040 inches in diameter. This is not a standard size wire, since it is larger than typical electro-discharge machining (EDM) wire. This results in pore sizes of approximately 200 microns; which would be sufficient for the scandium particles to transport to the emitter surface.

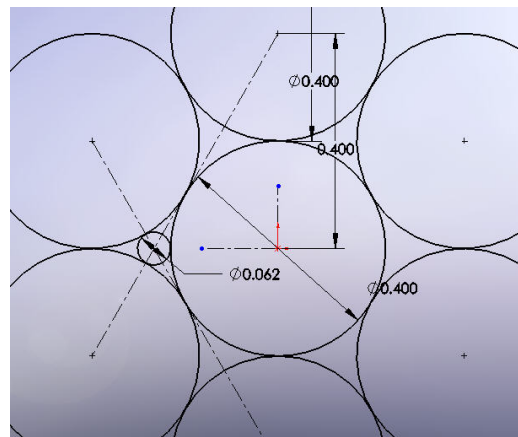


Figure 5. Relationship between diameter pore clearance and wire size in tungsten wire cathodes (Units are mm). This figure indicates that 400 micron diameter wire will allow passage of 62 micron diameter particles.

The purpose here was to determine if the 30-60 micron diameter particles would diffuse through the pores to the emission surface.

There was some expectation that the larger particles of scandium would result in transport to the surface in smaller pore size cathodes. The melting point of scandium is approximately 1600° C. While the emission surface temperature of cathodes is approximately 1000° C, the temperature near the heater is considerably higher. Since the reservoir in CCR's cathodes is adjacent to the heater, it is conceivable that scandium will vaporize in the reservoir and subsequently condense on the cathode surface after diffusing through the pores. Either transport mechanism would replenish scandium on the emission surface.

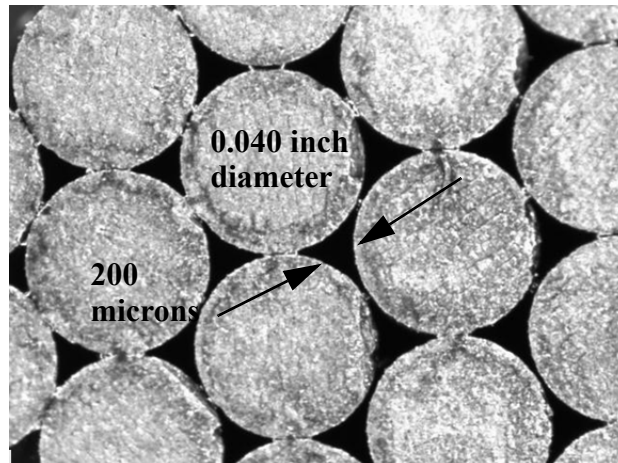


Figure 6. Sintered tungsten wires of sufficient size to allow propagation of 40 micron diameter scandium particles.

Unfortunately, sufficiently large sections of the larger diameter wire could not be adequately sintered. Note in Figure 6 that the tungsten wires are only marginally bound together. When an attempt was made to slice the wire sections to form the reservoir cap, the structure disintegrated into individual wires. Two attempts were made to sinter large diameter wire with the available furnace facilities. Both attempts failed.

Fortunately, sintering of smaller wires appropriate for actual cathodes is routinely achieved. The failure of the planned experiment with the larger size scandium particles and large diameter wire does not indicate there will be a problem with standard size materials. CCR still has high confidence that this technique will be successful, though one cannot conclude the feasibility was clearly demonstrated. Still, there were no indications during the phase I program that this approach would not succeed.

Task 2. Investigate sintering of scandium wires with tungsten wires to form the cap of reservoir cathodes.

A tungsten wire cathode was constructed that included scandium in the cathode material. The Phase I proposal indicated that scandium wires would be interspersed with tungsten wires in the cathode structure. During the initial research, it was determined that scandium foil was available, so both wires and foil were obtained. The foil was 0.1 mm thick, and 1 square inch was obtained. Approximately 40 meters of 0.65 mm of scandium wire was also obtained.

The approach was to incorporate the scandium material within the tungsten material and look for enhanced emission along the interface. Parts were designed and procured for wire winding and sintering. Initial efforts to wind tungsten and scandium wires was not successful. Inhomogeneity and brittleness of the scandium wire caused it to break while winding.

The foil, however, was successfully integrated into a tungsten wire structure. Because it was not possible to achieve sufficient temperature for sintering the tungsten without melting the scandium, the scandium was used as a braze alloy. The structure was fired in a furnace at 1650° C for 15 minutes. The resultant structure was sectioned to determine if the scandium flowed sufficiently to leave the pores open while binding the adjacent tungsten wires. A photograph of the face is shown in Figure 7.

A number of scanning electron microscope (SEM) photographs were taken of this surface and are shown in Figure 8. One can see the basic wire structure from the photo near the edge. More importantly, however, are the photos showing a uniform distribution of pores over the surface. This indicates that the scandium flowed sufficiently to avoid plugging holes through which barium must be transported from the reservoir.

The face was analyzed using Energy Dispersive X-ray Analysis (EDAX) to confirm the presence of scandium. These results, shown in Figure 9, confirm the presence of scandium. Surprisingly, however, the analysis also indicates significant amounts of copper, though copper was not used anywhere in this material or the fixturing. Materials used in the structure were analyzed and results confirm insignificant levels of copper in the materials. It is now suspected that the copper originated from the brass EDM wire used to section the cathode. Future sectioning will use tungsten EDM, and the resultant surface will be reanalyzed to look for copper.

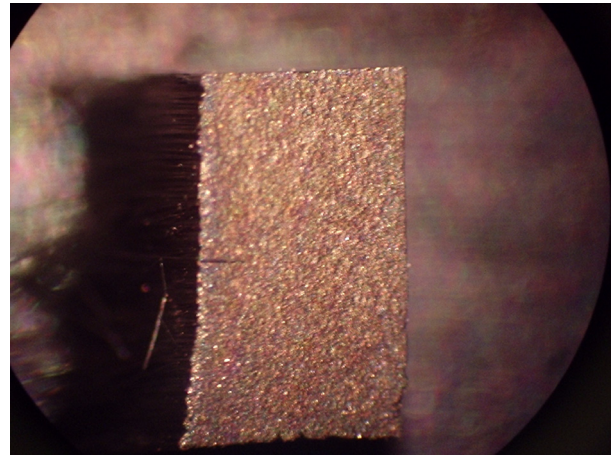


Figure 7. Face of tungsten wire assembly brazed with scandium

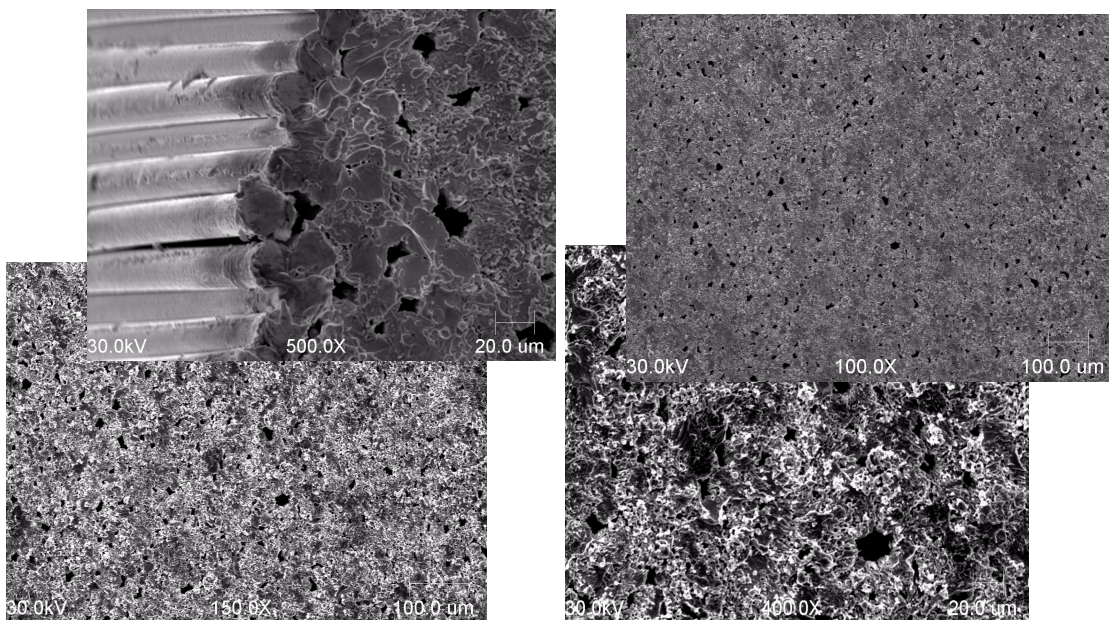


Figure 8. Scanning electron microscope photos of scandium brazed tungsten wire structure at different magnifications. Dark spots indicate pores through the material.

Results indicate that this is an effective technique for incorporating scandium into the structure of a tungsten wire reservoir cathode. Scandium is located between tungsten wires and on the surface of the pores. This should provide a robust source of scandium on the surface.

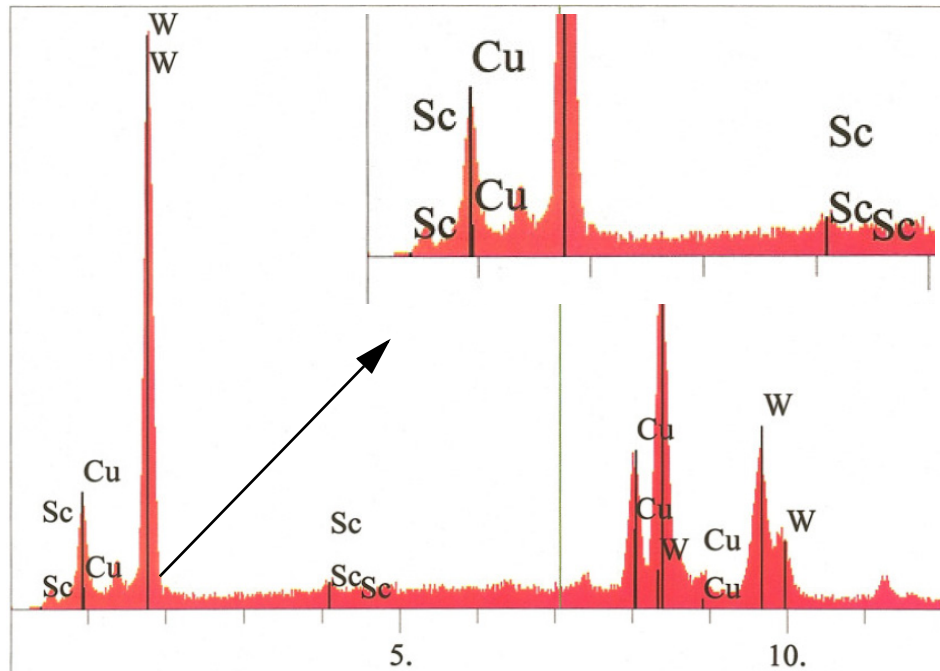


Figure 9. Spectrum analysis of scandium brazed tungsten wire surface

Task 3. Thick sputtering of scandium

Following discussions with HeatWave Labs, Inc., a subcontractor on the program, it was decided to pursue two additional approaches for fabrication of scandium cathodes: one is a chemical vapor infiltration (CVI) / chemical vapor deposition (CVD) process and the other is a proprietary process. CVI relies on gaseous diffusion to get the scandium into the pores of the substrate. The smaller the pores, the more challenging the task. The proprietary process uses a different mechanism to inject the scandium and is better suited for materials with very small pores. With the CVI process, the scandium will not penetrate deeply into the surface structure, which is desirable for this application. The proprietary process allows much deeper penetration. Both of these processes are actually quite simple and use existing equipment and technology. The only thing new is that the deposited/injected material contains scandium instead of some other metal.

As mentioned in Section 1, surface deposition of scandium was tried before; however, the deposited layer was thin and eroded away in time. The process here deposits much more material and allows significant penetration into the surface layer. The goal was to insert relatively significant quantities of scandium into the pores without completely closing them.

In Phase I, experiments were performed with deposition into a porous tungsten structure, since a tungsten wire cathode was not available for this experiment. The successful results, described here, have implications for both tungsten wire cathodes and traditional porous tungsten cathodes. It appears that the process could work for either cathode structure, significantly broadening the potential application.

During an approximately three-week period from mid February through March 8, Ultramet (Pacoima, CA) performed feasibility experiments using their chemical vapor deposition (CVD) process to deposit Sc_2O_3 coatings onto tungsten substrates provided by HeatWave Labs. Scandium infiltration runs were performed using an organometallic scandium precursor. Initial tests with the precursor demonstrated that it undergoes a violent exothermic reaction upon heating to 240 °C, even in an inert environment. The reaction was performed in a thermogravimetric analyzer/differential scanning calorimeter (TGA/DSC), and the weight loss was consistent with conversion of the precursor to scandium oxide (Sc_2O_3). X-ray diffraction of the reaction product confirmed it to be Sc_2O_3 .

Recall that previous investigators used scandium oxide to enhance the emission properties of the cathode. Consequently, Ultramet determined that scandium oxide would be both easier and more effective than scandium metal. Subsequent runs were performed in a small batch reactor, but with only one disk. Only small amounts of precursor were used for safety reasons, but this failed to deposit a measurable amount of coating. In a subsequent run, the amount of precursor was increased, and scandium oxide was detected on the surface of the disk via energy dispersive spectroscopy (EDS). XRD of the surface confirmed the composition to be Sc_2O_3 .

Figure 10 shows the levels of constituent materials from a section of a porous tungsten surface subjected to scandium oxide (Sc_2O_3) deposition. Note that the surface remains extremely porous, indicating that the process will not inhibit transport of barium to the surface. Measurement indicated that more than 5% by weight of the material is scandium oxide. The EDAX spectrum is shown in Figure 11

Spectrum processing:
No peaks omitted

Processing option: All elements analyzed (Normalised)
Number of iterations = 4

Standard:

C CaCO3 1-Jun-1999 12:00 AM
O SiO2 1-Jun-1999 12:00 AM
Sc Sc 1-Jun-1999 12:00 AM
Zn Zn 1-Jun-1999 12:00 AM
W W 1-Jun-1999 12:00 AM

Element	Weight%	Atomic%
C K	6.42	26.32
O K	15.37	47.29
Sc K	5.33	5.84
Zn K	2.14	1.61
W M	70.74	18.94
Totals	100.00	

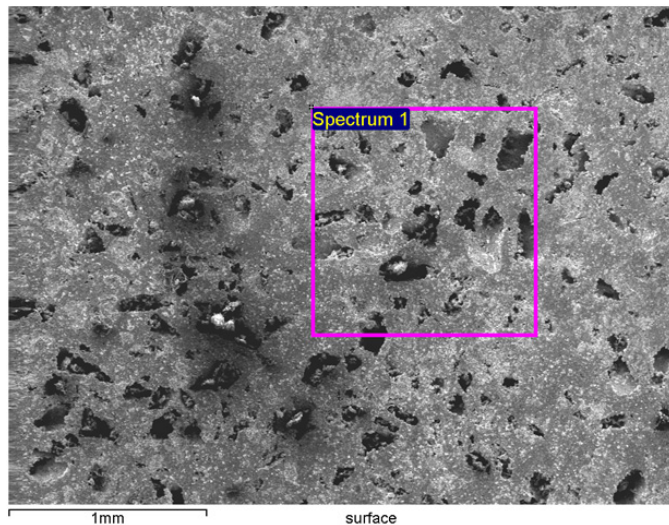


Figure 10. SEM and constituents of porous tungsten cathode section implanted with scandium. Measurement were taken from the region shown by the magenta square.

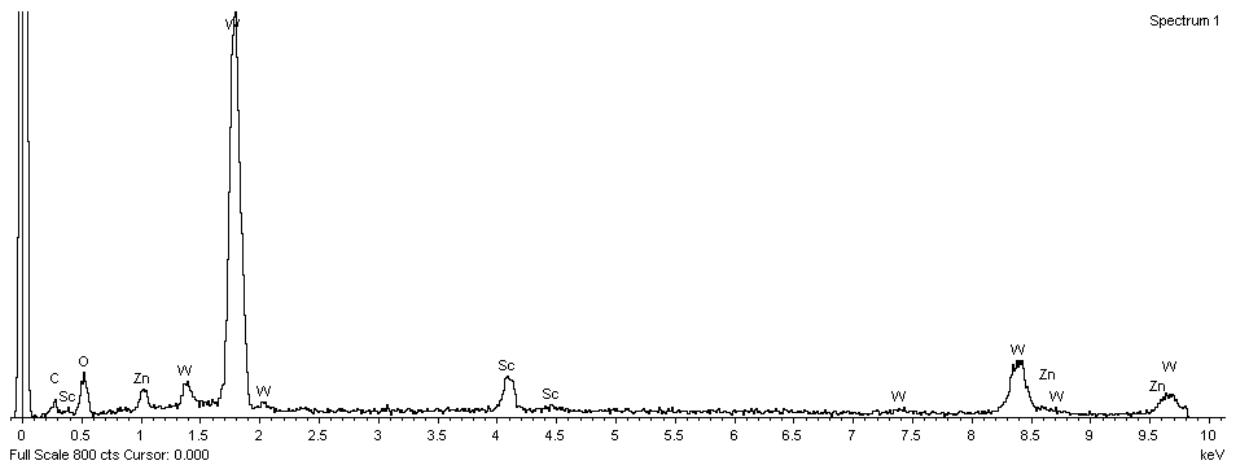


Figure 11. EDAX spectrum of surface regions indicated in Figure 10

Figure 12 shows another surface section, focusing on a surface feature. The spectrum of the region is shown in Figure 13. Note that this is clearly defined as a region of high scandium oxide concentration. Recall that Yamamoto deposited approximately 5% scandium on the surface.

Spectrum processing:
No peaks omitted

Processing option: All elements analyzed (Normalised)
Number of iterations = 4

Standard:

C CaCO₃ 1-Jun-1999 12:00 AM
O SiO₂ 1-Jun-1999 12:00 AM
Sc Sc 1-Jun-1999 12:00 AM
W W 1-Jun-1999 12:00 AM

Element	Weight%	Atomic%
CK	5.69	11.98
OK	39.04	61.76
Sc K	43.84	24.68
WM	11.43	1.57
Totals	100.00	

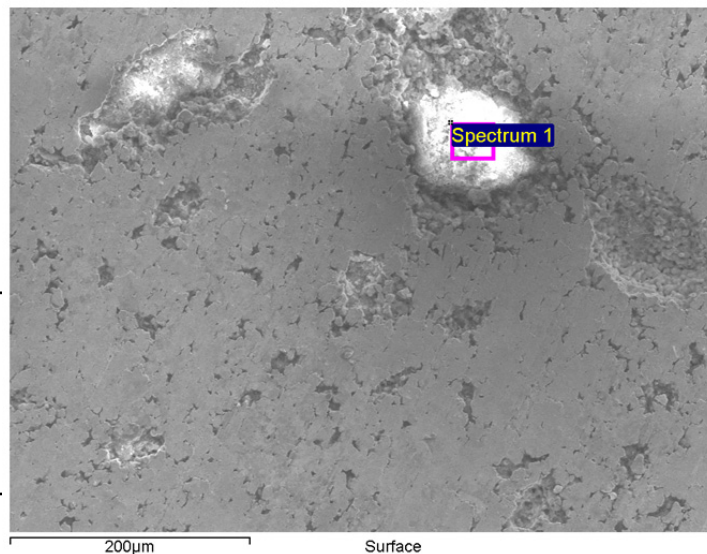


Figure 12. SEM and analysis of region of scandium deposition on the surface of a porous tungsten cathode.

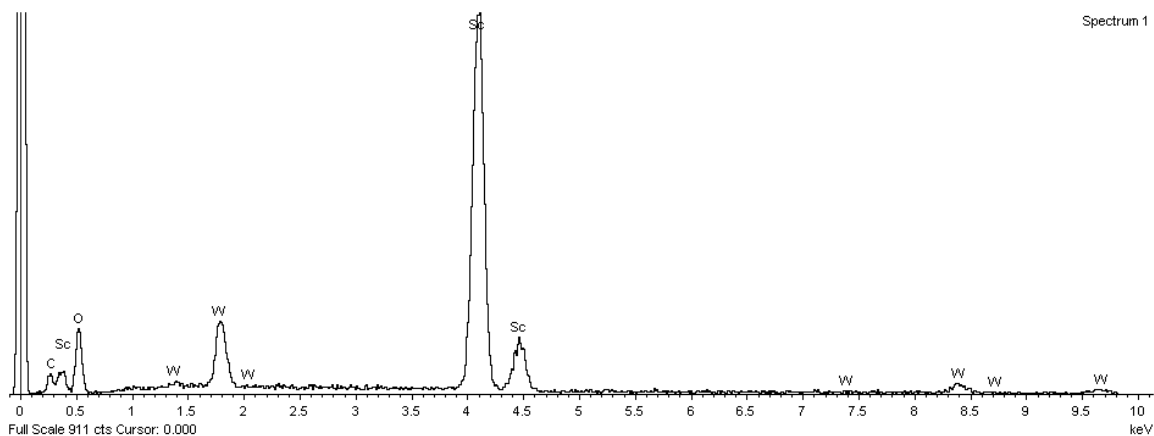


Figure 13. Spectrum analysis of cathode surface shown in Figure 12

Figure 14 shows the analysis results of the same cathode section as Figure 12 but displaced from the feature shown in Figure 12 and 13. The analysis shows mostly all tungsten with approximately 2% scandium oxide, implying that the feature shown in Figure 12 is primarily scandium oxide. The associated spectrum is shown in Figure 15.

Spectrum processing:
No peaks omitted

Processing option: All elements analyzed (Normalised)
Number of iterations = 3

Standard:

C CaCO₃ 1-Jun-1999 12:00 AM
O SiO₂ 1-Jun-1999 12:00 AM
Sc Sc 1-Jun-1999 12:00 AM
W W 1-Jun-1999 12:00 AM

Element	Weight%	Atomic%
CK	2.53	15.53
OK	10.09	46.49
ScK	2.38	3.90
WM	85.00	34.09
Totals	100.00	

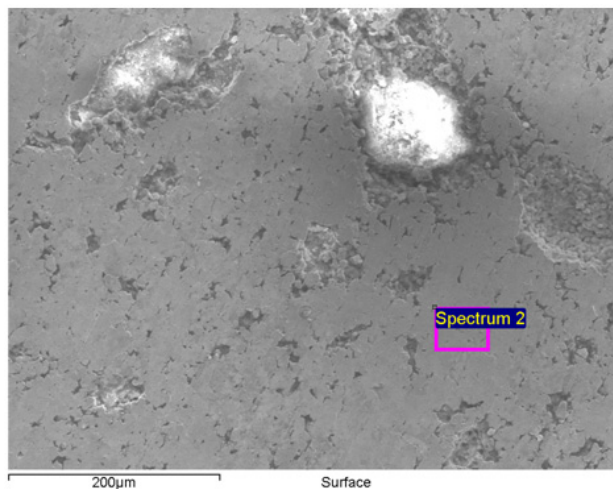


Figure 14. SEM and surface analysis of region away from surface feature analyses in Figures 12 and 13

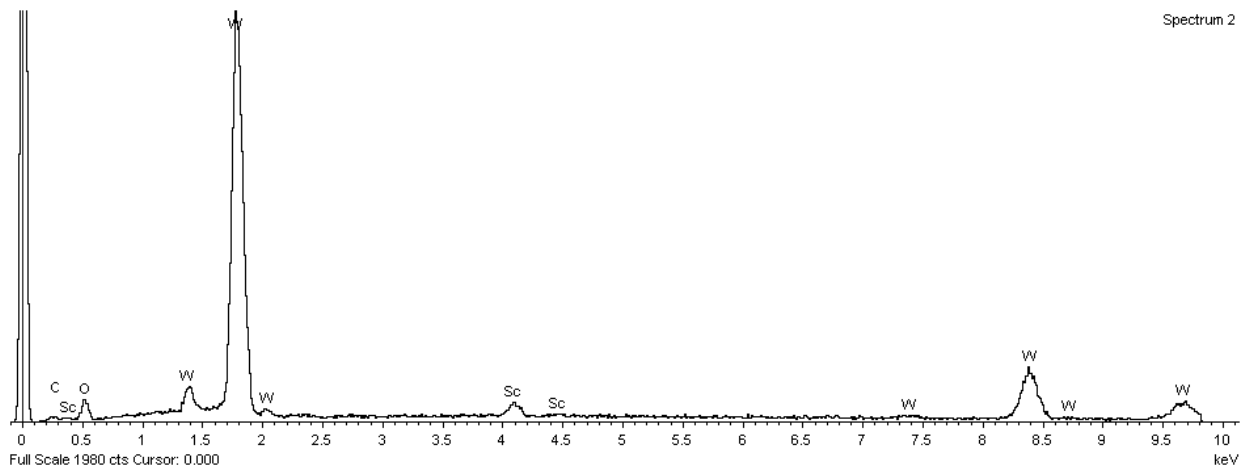


Figure 15. Spectrum away from surface feature shown in Figure 14

Figure 16 shows the same measurement from a sliced section of the cathode. The spectrum is shown in Figure 17. This is a subsurface section of the cathode, indicating appreciable penetration, approximately 20 microns. In this analysis, more than 6% by weight of the material in the region analyzed is scandium oxide. This clearly demonstrates that significant amounts of scandium oxide can be deposited on and below the surface of cathodes using the Ultramet process. Four additional samples were infiltrated with scandium oxide via a modified process designed to increase the scandium's depth of penetration. Surface EDS of the disks shows increased amounts of scandium oxide in the surface. Cross sectional analysis indicates that scandium oxide was deposited approximately 1 mm below the surface. Such penetration is unprecedented for scandium oxide and exceeds the requirements of the program.

Spectrum processing :
No peaks omitted

Processing option : All elements analyzed (Normalised)
Number of iterations = 4

Standard :
C CaCO3 1-Jun-1999 12:00 AM
O SiO2 1-Jun-1999 12:00 AM
Sc Sc 1-Jun-1999 12:00 AM
Zn Zn 1-Jun-1999 12:00 AM
W W 1-Jun-1999 12:00 AM

Element	Weight%	Atomic%
CK	40.50	65.08
OK	24.02	28.98
Sc K	6.84	2.94
Zn K	0.00	0.00
WM	28.64	3.01
Totals	100.00	

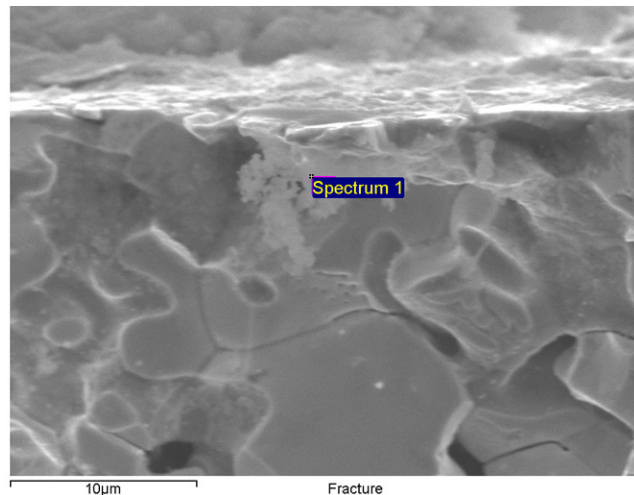


Figure 16. SEM and analysis of sliced section of porous tungsten cathode implanted with scandium. The measurements were made in the rectangular section mostly hidden by the “Spectrum” notation.

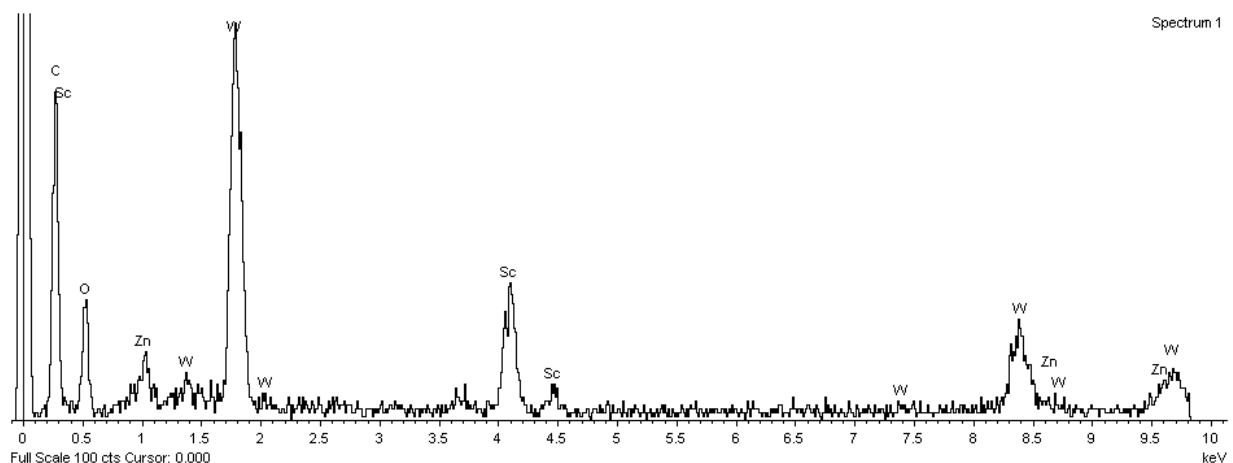


Figure 17. Spectrum of subsurface material from region shown in Figure 16.

This task successfully deposited scandium oxide on and below the surface of a porous tungsten cathode using the CVI/CVD process. The surface feature analyzed in Figures 12 and 13 is approximately 50 microns in diameter. Such a deposit could survive substantially more ion bombardment or other removal processes than the nanoparticles used in the Chinese approach. In addition, the subsurface deposits of scandium oxide could provide a continuing source of scandium.

Task 4. Design a photonic bandgap traveling wave tube incorporating a high current density scandate cathode

The Phase I program explored several concepts for advanced slow wave structures for W-Band amplifiers. MIT took the lead in performing this research. The selection of a specific structure was needed to define the size of the electron beam. The advanced structure would use a high current density, scandate cathode that would be built and tested in a Phase II program. A major goal of the advanced structure was to achieve a design that would allow an electron beam with the largest possible diameter, consistent with high gain, bandwidth, and efficiency at W-Band. The research concentrated on photonic structures, which have been identified in previous research as promising for supporting high order modes with a relatively large beam tunnel.

Introduction

There are multiple challenges to building an interaction structure for a slow wave device at millimeter and sub-millimeter wave frequencies. The first and foremost challenge arises from the sub-wavelength transverse and axial dimensions of the circuit. The typical circuit parameters for a 94 GHz TWT design with a ladder-type interaction structure are shown in Table 1.

The operating current is limited by the band edge oscillation thresholds as well as the thermal capability of the small circuit to tolerate beam interception. These challenges are well documented in the literature. An example of a successful design is the ladder-type, slow wave structure (SWS) in the Millitron Series of tubes manufactured by Communications & Power Industries, Inc.

Frequency	94 GHz
Voltage	25 kV
Beam Current	0.2 A
Perveance	0.05 μ P
Axial Period	0.81 mm
Beam Diameter	0.5 mm
Beam Tunnel Diameter	0.6 mm
Focusing Field (2.5 x Brillouin Field)	0.3 Tesla
Cavity Dimensions	$\sim 3.7 \times 1.9$ mm
Coupling Slot Dimensions	1.5 x 0.5 mm
Gain for synchronous case	23.3 dB/cm

Table 1. Main parameters of a typical 94 GHz TWT with a ladder type interaction circuit operating in the TM₁₁₀ mode.

Circuit fabrication will be easier and less expensive and the circuit's thermal capability will considerably improve if the transverse dimensions of the circuit are larger and the beam tunnel size increased. The transverse circuit dimensions of the beam tunnel are dictated by the operating wavelength for conventional fundamental mode interaction structures. The recent advent of frequency selective, PBG structures offers new possibilities for building an improved slow wave structure at millimeter wave frequencies.

In previous research under an Innovative Vacuum Electronics Multidisciplinary University Research Initiative (MURI) funded by the Air Force Office of Scientific Research (AFOSR), MIT demonstrated that a gyrotron PBG resonator allows higher order mode operation with dramatic suppression of parasitic modes, both above and below the operating frequency [18].

The overmoded, PBG interaction structure for a 94 GHz traveling wave tube (TWT) will mitigate many of the problems faced in a conventional 94 GHz TWT circuit. The circuit is amenable for fabrication using modern fabrication techniques, such as wire EDM or another micro-fabrication techniques. The electron beam was chosen such that the electron gun could be fabricated with a high current density scandate cathode.

Design of the Slow Wave Structure

The novel, overmoded, PBG interaction circuit is a derivative of the ladder-type SWS, but with the following advantages:

- the circuit operates in the TM₁₃₀ mode, which increases the linear transverse dimensions by a factor of approximately three,
- the beam tunnel diameter is 1.5 times the diameter of the conventional beam tunnel listed in Table 1,
- the circuit reduces the impedance at the band edges due to the unique properties of the PBG structure. This will increase the threshold of the band edge oscillations.

A schematic of the interaction structure is shown in Figures 18 and 19. The central section consists of a rectangular cavity coupled to its neighboring cavities through rectangular slots, shown in green. The coupling slots are staggered so that they alternate between the top and bottom of each cell. The side walls of the cavity are formed by a PBG structure which, in this case, consists of a periodic array of square posts. This makes the walls grating-like. The PBG structure acts as an efficient reflector for a band of frequencies around the operating frequency of 94 GHz and acts as a transparent wall at lower and higher frequencies. The central dimensions of the cavity are chosen so the TM_{130} mode is resonant at 94 GHz. The coupling slots allow a traveling wave with a passband of approximately 3 GHz to propagate in the circuit.

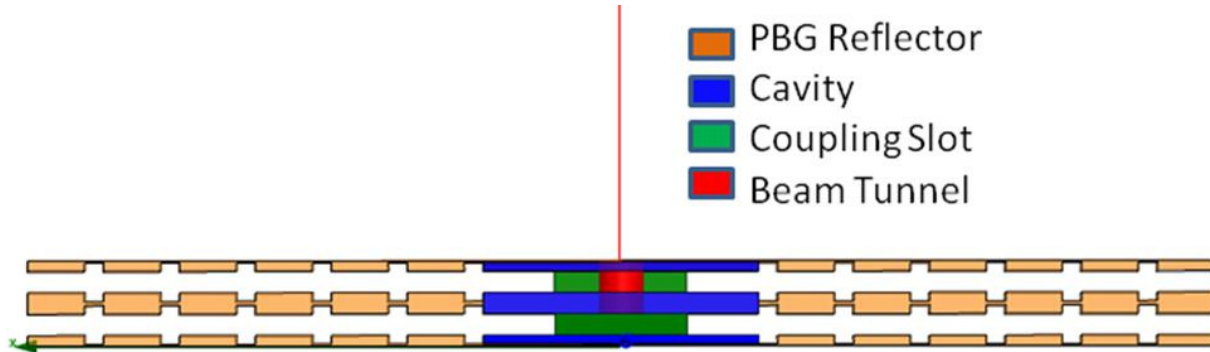
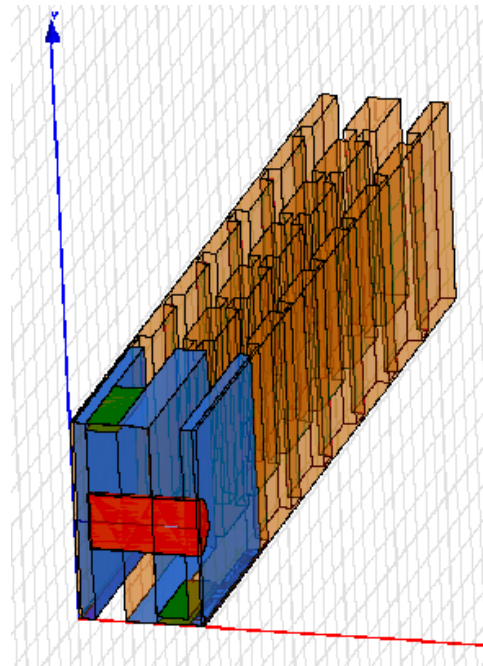


Figure 18. Top view of the PBG interaction structure showing a full central cavity and two adjacent half cells. A part of the beam tunnel (shown in red) is obscured by the coupling slot (shown in green). All of the colored regions correspond to the vacuum region of the interaction structure.

The frequency selective properties of the PBG structure will prevent good confinement of the lower order modes, such as the TM_{120} and TM_{110} . This dramatically reduces their coupling to the electron beam. This results in a reduced interaction impedance for the lower order modes, discussed below. The dispersion diagram of the SWS is shown in Figure 20. Of the two lower order parasitic modes, namely the TM_{110} and TM_{120} , only the former is marginally confined in the

Figure 19. Isometric view of the PBG interaction structure (split in half along the YZ plane) showing a full central cavity and two adjacent half cells. The electron beam travels through the beam tunnel (red) in the z direction.



structure. The electron beam line is shown for a 40 kV beam voltage with the operating point at 94 GHz in the TM_{130} mode.

Figures 21 and 22 show High Frequency Structure Simulator (HFSS) simulations of the operating mode in the SWS. The operating mode is well confined in the central part of the cavity due to strong reflection from the PBG structure forming the side walls. The lower and higher order parasitic modes do not exhibit this feature and will leak through the side walls, thus significantly lowering their coupling to the electron beam. The interaction impedance of the parasitic TM_{110} mode is only 0.2 ohms, which is a factor of 13 times lower than the impedance of the operating TM_{130} mode, as shown in Figure 20. The interaction impedance versus phase for the operating TM_{130} mode was calculated and is shown in Figure 23.

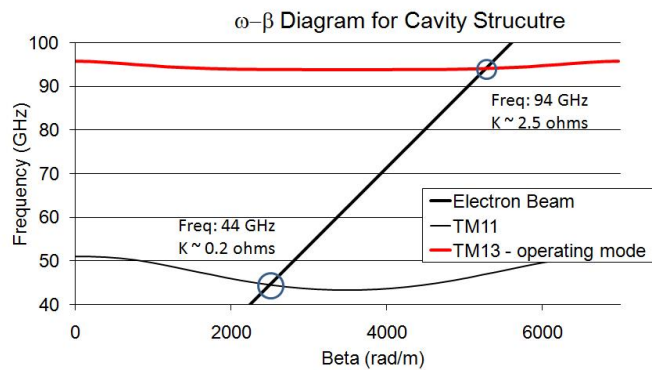


Figure 20. Dispersion diagram for the slow wave structure. The TM_{130} operating mode is shown in red. The lower frequency TM_{110} parasitic mode is shown in black. Also shown is the electron beam line for a 40 kV beam. The circuit is operated in the first forward space harmonic corresponding to 270 degrees phase advance between two adjacent cells.

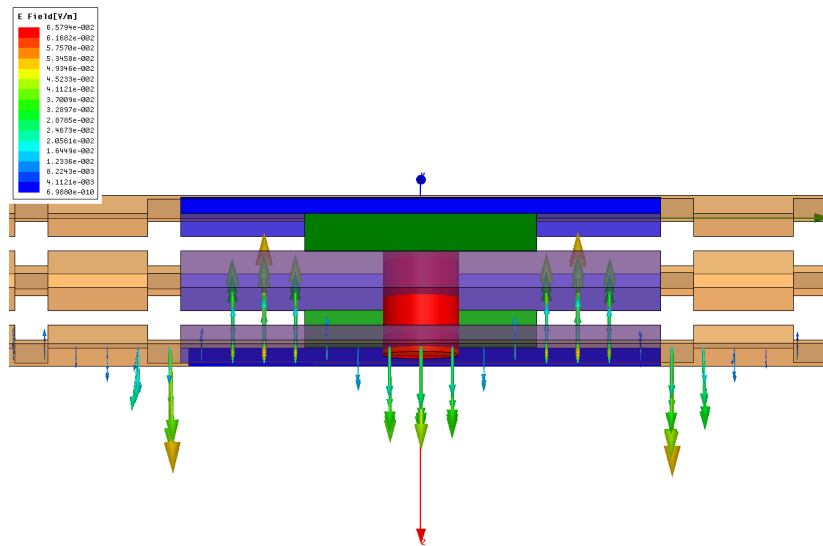


Figure 21. HFSS simulation of the operating mode (TM_{130}) in the slow wave structure. The field has three variations in the central part of the cavity.

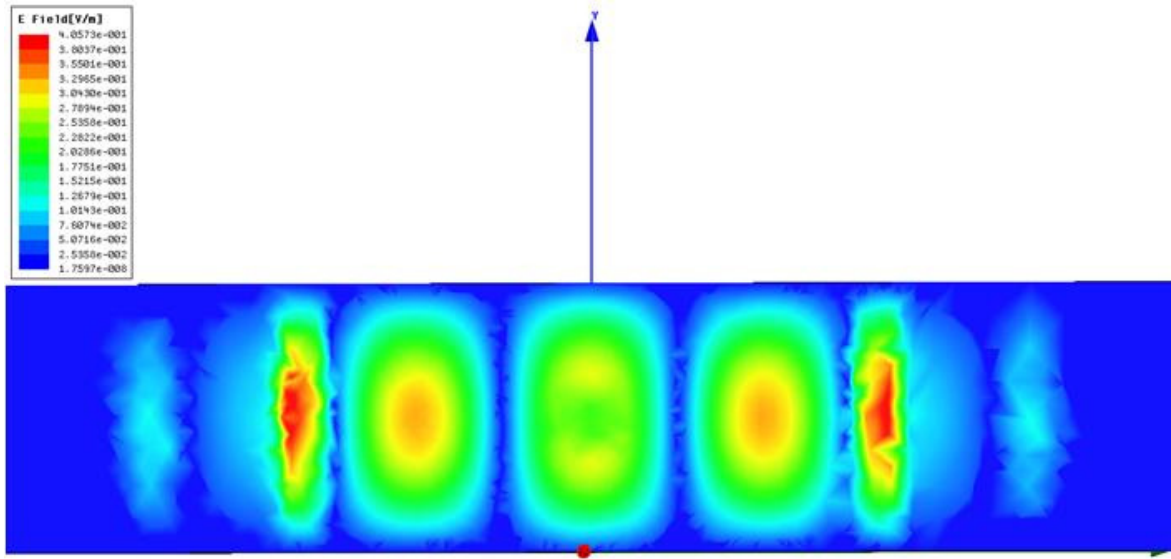


Figure 22. HFSS simulation of the operating mode (TM_{130}) in the slow wave structure. The field has three variations in the central part of the cavity and is well confined by the PBG sidewalls.

The design uses a 40 kV, 1 A electron beam of diameter 0.8 mm. The current density in the circuit is approximately 200 A/cm^2 . This current density is at the upper limit of projected scandate cathode current densities. If the cathode could work at this current density, operation with no beam compression would be possible; however, it may be more practical to operate the first device with a modest area compression of approximately 4. The cathode

current loading would be 50 A/cm^2 , which should be consistent with the scandate cathodes being considered for the electron gun. The Brillouin field for the chosen electron beam is 0.14 T; using 2.5 times the Brillouin field implies a 0.3 T field will be required in the circuit. The calculated gain for the PBG TWT synchronous case is 9.2 dB/cm. This is a lower value of gain than in a fundamental TWT but is sufficient for achieving high power output. A comparison of the conventional TWT design described in Table 1 and the proposed PBG TWT design is shown in Table 2.

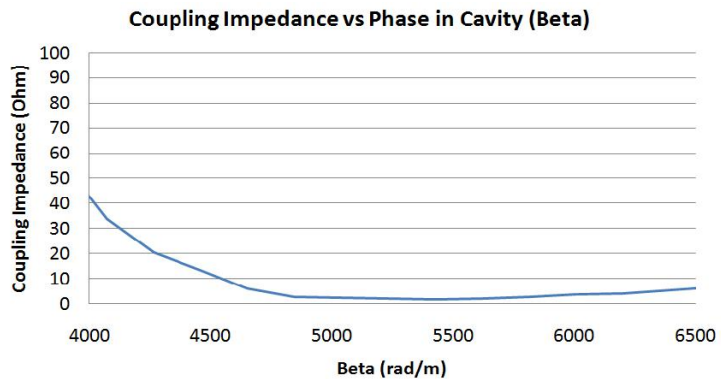


Figure 23. Interaction impedance of the operating mode (TM_{130})

	Conventional TWT Design	Overmoded PBG TWT Design
Frequency	94 GHz	94 GHz
Voltage	25 kV	40 kV
Beam Current	0.2 A	1.0 A
Perveance	0.05 μP	0.125 μP
Axial Period	0.81 mm	0.89 mm
Beam Diameter	0.5 mm	0.8 mm
Beam Tunnel Diameter	0.6 mm	0.9 mm
Focusing Field (2.5 x Brillouin)	0.3 Tesla	0.3 T
Cavity Dimensions	$\sim 3.7 \times 1.9$ mm	$\sim 6 \times 3$ mm
Coupling Slot Dimensions	1.5×0.5 mm	$\sim 1.4 \times 0.2$ mm
Gain for synchronous case	23.3 dB/cm	9.2 dB/cm

Table 2. Comparison of a typical 94 GHz TWT based on a ladder type interaction circuit with an overmoded PBG TWT.

Overmoded Coupled Cavity TWT Structure

The last phase of the work examined a simpler structure that is overmoded and uses dielectric loading in selective locations to damp the lower order modes. This structure is shown in Figure 24, and the relevant dimensions are listed in Table 1. The structure can be fabricated as an overmoded folded waveguide, as shown in Figure 24, or the coupling slots can be rotated 90 degrees and the structure is amenable to fabrication as a ladder circuit. Further discussion in this report will be limited to the folded waveguide like geometry, though similar results can be achieved with the ladder type geometry.

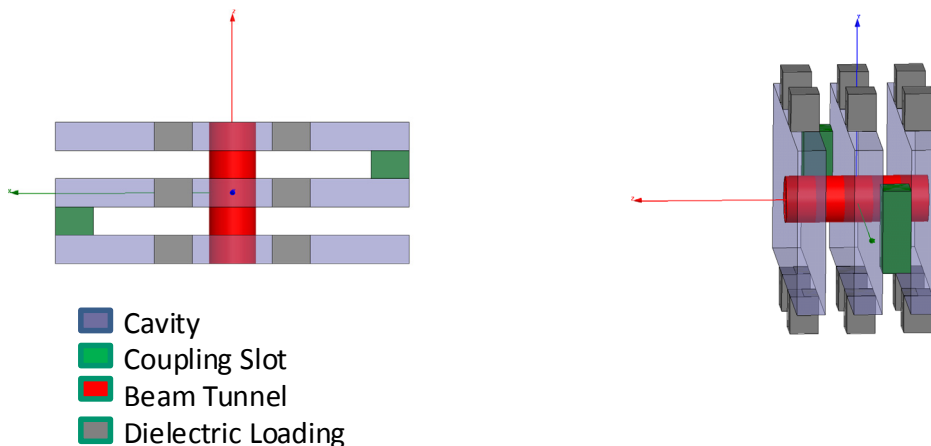


Figure 24. Geometry of the coupled cavity TWT. Three cavities are coupled together by two slots on opposite side of the cavity. The beam tunnel shown in red passes through the center of each cell.

Table 1. Dimensions of TWT Cavity

Attribute	Dimension
Beam Tunnel Diameter	0.7 mm
Cavity Size	5.6 mm x 2.65 mm x 0.4 mm
Slot Size	1.3 mm x 0.6 mm x 0.4 mm

The structure supports a TM_{311} mode and, in the current configuration, has a single beam tunnel. The structure can also support three beam tunnels located on the three maxima of the mode. The choice of beam tunnels can lead to additional mode selectivity, for instance having the beam in the two outer beam tunnel (not shown in Fig. 24) will allow greater coupling to the TM_{311} mode while reducing the coupling to the TM_{111} mode, which has a field maximum at the center of the cavity. This overmoded circuit will thus allow operation at higher beam current with lower perveance, which provides the advantages of a sheet beam device without the complication of a high aspect ratio sheet beam.

The structure resembles an overmoded folded waveguide loaded with lossy dielectric at the null point of the TM_{311} mode to minimize the effect of the loading on the operating mode. The lower order modes namely the TM_{111} and TM_{211} , have significant field amplitude at the location of the dielectric and hence are significantly damped.

Figure 25 shows an overmoded TM_{311} cavity with the proposed dielectric loading. The structure is modeled with HFSS. Shown in Figure 26 is the effect dielectric loading on the transmission through the coupled cavity circuit. An artificial dielectric material with an epsilon of approximately 20 and tan delta of approximately 0.25, available from the Ceradyne, Inc., was used in the simulations. The main parasitic modes, TM_{111} and TM_{211} , exhibit significant losses compared to the operating TM_{311} mode. Though the TM_{121} mode has lower loss than other parasitic modes, the location of the electron beam is not optimal for this mode, and hence it is not favored.

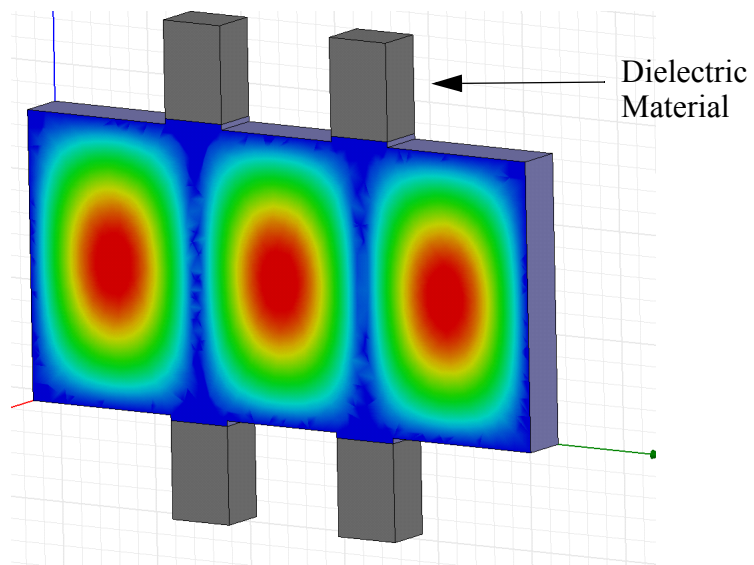


Figure 25. HFSS simulation of a single structure of the interaction structure showing the location of the dielectric loading minimally perturb the operating mode.

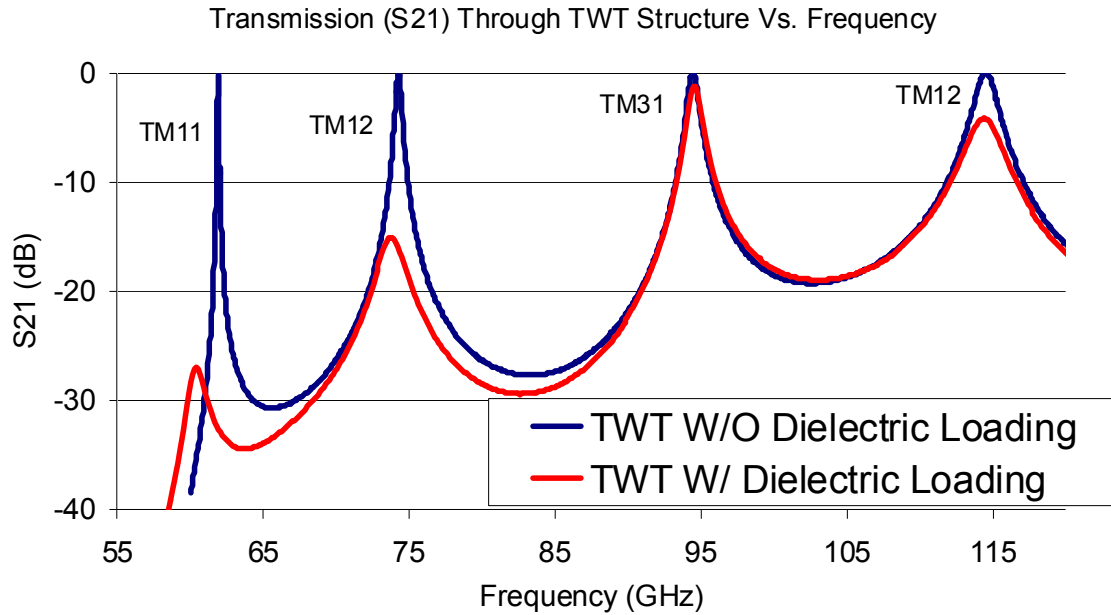


Figure 26. Transmission through a three cell cavity structure, modeled in HFSS showing high losses for the parasitic modes compared with the operating TM311 mode

The cold dispersion of the interaction structure is shown in Figure 27.

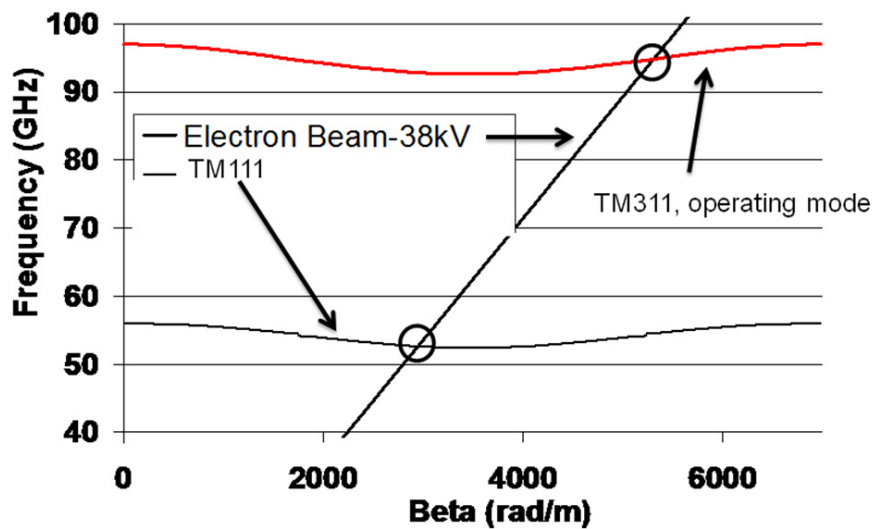


Figure 27. Cold dispersion diagram of the interaction structure. The TM211 mode is not shown because its coupling to the beam is extremely weak.

With the cavity mode and dimensions fixed, an appropriate coupling mechanism between cavities was chosen. Figure 24 shows three coupled cavity cells to illustrate the TWT's geometry. Coupling is determined by the dimensions of the beam tunnel and the addition of coupling slots on opposite sides of the cavity. This geometry was chosen for its ease of fabrication and its

wideband dispersion characteristics. As seen in Figure 26, the TM_{311} mode interacts with the beam over a 3 GHz passband. The interaction impedance, K , is approximately 20 Ohms over this operating region, which corresponds to a gain of 12 dB/cm for a 40 kV, 1 A beam.

Numerical Simulations

Due to the unconventional (overmoded and multiple beams) nature of the circuit, it is not straightforward to use existing coupled cavity TWT codes, such as Christine-CC, to model the circuit. Preliminary estimates of linear gain were performed using Pierce type theory. The gain was calculated to be about 12 dB/cm for a 40 kV, 1 A electron beam through the central tunnel.

Advanced simulations used MAGIC, a full 3D PIC code, to study the beam wave interaction and parasitic oscillations. A MAGIC model of a nine cell structure is shown in Figure 28. MIT successfully verified that, for the

operating current of 1 A, the structure is zero drive stable. Oscillations in the TM_{111} mode were observed at beam currents over 5 A, and tens of kW of power were recorded. As expected oscillations in the TM_{211} mode were not observed, because the coupling of the electron beam to the TM_{211} and TM_{121} modes is extremely weak.

MIT is conducting further simulations to show gain in the operating mode and verify the estimates from the Pierce type theory

Conclusion

The Phase I program successfully completed a preliminary design of an overmoded TWT with a photonic (PBG) structure. The preliminary PBG structure design allows an increase of 50% in beam tunnel diameter relative to a conventional ladder-type structure. Detailed HFSS simulations show the characteristics of the operating mode (TM_{130}) in the slow wave PBG structure. The dispersion diagram was calculated for the design mode in the PBG structure and for the competing lower order modes. The results demonstrate that it should be feasible to operate in the design mode without parasitic oscillations in the unwanted modes. A 40 kV, 1 A electron beam with a diameter of 0.8 mm was used in the design. For an area compression factor of 4, the electron beam requires a cathode with 50 A/cm^2 current density, which is consistent with the goals of the program. Though the gain per unit length is lower in the PBG TWT, the gain is calculated to be 9 dB/cm, which is acceptable. Higher gain may be achieved with further optimization of the structure. The PBG structure can be tuned to reduce the impedance at the band edges and increase the oscillation thresholds at these points. This should allow operation at higher beam current and increased device gain. The larger circuit beam tunnel not only allows a larger size electron beam, relaxing the constraints on the electron gun design, but also allows larger transverse dimensions, which increase the thermal handling capability.

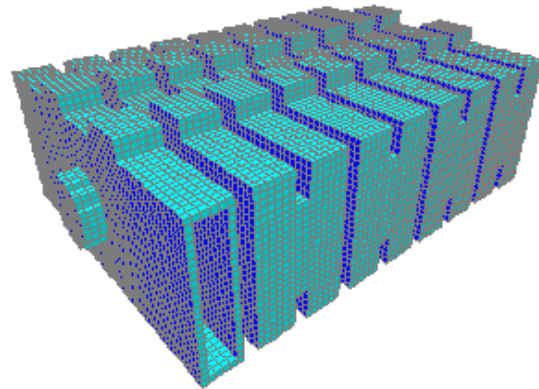


Figure 28. Model of nine cells of the structure in MAGIC

MIT also completed the proof-of-principle design of an overmoded traveling wave interaction circuit for a W-band TWT predicted to operate in the TM_{311} mode while being stable at the lower order modes. The structure can also be used with multiple beams, which has the advantages of using low perveance beams. The linear gain was calculated to be about 12 dB/cm for a single 40 kV, 1A beam using Pierce type theory. Full 3D PIC simulations are underway to determine the nonlinear gain. The 3D PIC simulations indicated that the structure does not self excite in the lower order modes.

3. Program Summary

The Phase I program demonstrated several techniques for implanting scandium into and on the surface of tungsten dispenser cathodes and providing replenishment mechanisms against typical erosion processes. This addresses a serious problem with scandate cathodes that have prevented their use in electron guns since their initial development more than twenty years ago. If successfully demonstrated, scandate cathodes would provide increased current density emission for the required lifetime for most applications. Each technique investigated appears feasible and would use existing facilities and equipment. To demonstrate the capability in an actual device, the program designed a photonic band gap TWT compatible with cathodes investigated in the Phase I program. Successful demonstration of these cathodes in an actual RF device, coupled with life studies of cathodes, would establish scandate cathodes as a viable electron source for future devices.

References

- [1] J. Hasker, J. Van Esdonk, and J.E. Crombeen, "Properties and manufacture of Top-Layer Scandate Cathodes," *applied Surface Science* 26, (1986), 173-195.
- [2] S. Yamamoto, S. Taguchi, I. Watanabe, and S. Kawase, "Electron Emission Properties and Surface Atom Behavior of an Impregnated Cathode Coated with Tungsten Thin Film Containing Sc_2O_3 ," *Japanese Journal of Applied Physics*, Vol. 25, No. 7, July 1986, pp. 971-975.
- [3] G. Lesny, R. Forman, "Surface Studies on Scandate Cathodes and Synthesized Scandates," *IEEE Trans. on Electron Devices*, Vol 37, No. 12, December 1990, pp. 2595-2604.
- [4] C. Crombeen and J. Hasker, "Some Experiments on the Role of Oxygen and Surface Reactions for Tungsten and Scandate Thermionic Emitters," *IEEE Trans. on Electron Devices*, Vol 37, No. 12, December 1990, pp. 2585-2588.
- [5] J. Hasker and C. Crombeen, "Scandium Supply After Ion Bombardment on Scandate Cathodes," *IEEE Trans. on Electron DEvices*, Vol. 37, No. 12, December 1990, PP 2589-2594.
- [6] R.S. Raju and C.E. Maloney, "Characterization of an Impregnated Scandate Cathode Using a Semiconductor Model," *IEEE Trans. on Electron Devices*, Vol. 41, No. 12, December 1994, pp. 2460-2467.
- [7] G. Graertner, D. Barratt, "Life-Limiting mechanisms in Ba-oxide, Ba-dispenser and Ba-Scandate cathodes, Proc. 5th International Vacuum Electron Sources Conference, September 2004, pp. 59-61.
- [8] A. Shih, J.E. Yater, and C. Hor, "Scandate Cathode Fundamentals: Interactions of Ba, O, and Sc on W," Proc. 5th International Vacuum Electron Sources Conference, September 2004, pp. 57-58.

- [9] R.L. Ives, L. Falce, S. Schwartzkopf, R. Witherspoon, "Controlled Porosity Cathodes From Sintered Tungsten Wires," *IEEE Trans. on Electron Devices*, Vol. 52, No. 12, December 2005, pp. 2800-2805.
- [10] M. Zhang, H. Zhang, P. Liu, and Y. Li, "Investigation of recovery characteristics after ion bombardment on scandate cathode," *Proc. 5th International Vacuum Electron Sources Conference*, September 2004, pp. 153-155.
- [11] W. Liu, K. Zhang, Y. Wang, K. Pan, X. Gu, J. Wang, J. Li, M. Zhou, "Operating Model for Scandate Cathode with Scandia Doped Tungsten Bodies," *Proc. 5th International Vacuum Electron Sources Conference*, September 2004, pp. 62-64.
- [12] D. Jiang, S. Hong, C. Zhou, D. Wang, X. Liu, "Preparation of Impregnated Barium Scandate Cathode and Its Application," *Proc. 5th International Vacuum Electron Sources Conference*, September 2004, pp. 206-207.
- [13] W. Shuguang, "Scandate Cathode for TWT," *Proc. 5th International Vacuum Electron Sources Conference*, September 2004, pp. 224-225.
- [14] H. Yuan, X. Gu, K. Pan, Y. Wang, W. Liu, K. Zhang, J. Wang, M. Zhou, J. Li, "Characteristics of scandate-impregnated cathodes with sub-micron scandia-doped matrices," *Applied Surface Science*, 251 (2005) pp. 106-113.
- [15] G. Schietrum, G. Caryotakis, N. Luhmann, Y. Wang, J. Li, G. Miram, B. Vancil, "100 A/cm² Tungsten-Scandate Nanopowder Thermionic Cathode Testing at SLAC," *Multidisciplinary University Research Initiative Annual Review*, Monterey, CA, April 2006.
- [16] M. Ravi, P. Devi, K. Kumar, K. Bhat, "Characterization of W-Ir Mixed Metal Matrix Scandate Cathode," *IEEE International Vacuum Electronics Conference and IEEE International Vacuum Electron Sources Conference*, Monterey, CA April 2006, pp. 57-58.
- [17] L. Falce, R.L. Ives, "Sintered Wire Cathode," U.S. patent application 11/085,425, March 2005.
- [18] "Photonic-Band-Gap Resonator Gyrotron," J. R. Sirigiri et al., *Phys. Rev. Lett.*, Vol. 86, No. 24, pp. 5628-5631 (2001)
- [19] George Miram, private communication, March 2007.
- [20] Computer Optimized Design of Electron Guns, DOE contract DE-FG02-06ER86276, June 28, 2006 through August 8, 2009.
- [21] George Miram, private communication, March 2007.
- [22] L. Garbini, N. Sun, and L. Falce, "A Method of Predicting Dispenser Cathode Performance by the Measurement of Barium Flux," *IEEE International Vacuum Electronics Conference and IEEE International Vacuum Electron Sources Conference*, Monterey, CA April 2006, pp. 207-208.
- [23] Sirigiri, J.R. Chen, C.; Shapiro, M.A.; Smirnova, E.I.; Temkin, R.J., "New opportunities in vacuum electronics using photonic band gap structures," *AIP Conference Proceedings*, n 625, 2002, p 151-7.
- [24] Improved Field Emitter Array Cathodes for Advanced RF Sources, U.S. Air Force Contract F33615-03-M-1509, completed May 2004.
- [25] E. I. Smirnova, C. Chen, M. A. Shapiro and R. J. Temkin, "Simulation of Photonic Band Gaps in Metal Rod Lattices for Microwave Applications," *J. Appl. Phys.* Vol. 91, No. 3, pp. 960-968 (1 Feb., 2002).
- [26] U.S. Department of Energy Small Business Innovation Research Grant DE-FG-04ER83918. August 2004 through July 2007.

- [27] B.H. Alexander and R.W. Balluffi, *Acta Met.*, 1957, 5 (11), 666-677.
- [28] Development of Confined Flow Multiple Beam Electron Guns for High Power RF Sources, U.S. Department of Energy Grant No. DE-FG03-00ER82964.
- [29] Lawrence Ives, "MEMS and FEAs for HF TWTs and BWOs," Tri-Services Vacuum Electron Devices Conference, Norfolk, VA, April 2003.
- [30] High Current Field Emitter Arrays for Directed Energy Weapons, U.S. Air Force Contract Number FA9550-06-C-0087, August 2006 - May 2007.
- [31] MEMS-based Traveling Wave Tube Amplifier for Space Applications, Phase II Air Force Research Lab SBIR, Contract Number F29601-03-C-0049, completed February 2007.
- [32] Advanced Backward Wave Oscillators, NASA contract No. NAS3-01014, Administered by NASA Glenn Research Center, January 2001- January 2004.
- [33] Meander Line Traveling Wave Tube THz Amplifier, U.S. Air Force contract FA9550-05-C-0105. Phase II initiated January 1, 2007.